Society For Biomaterials

Influence of oxidative nanopatterning and anodization on the fatigue resistance of commercially pure titanium and Ti–6Al–4V

Amirhossein Ketabchi,[1] Arnaud Weck,[1,2] Fabio Variola[1,2]

[1]Department of Mechanical Engineering, University of Ottawa, Ottawa, Ontario, Canada K1N 6N5
[2]Department of Physics, University of Ottawa, Ottawa, Ontario, Canada K1N 6N5

Received 12 November 2013; revised 31 March 2014; accepted 22 May 2014
Published online 00 Month 2014 in Wiley Online Library (wileyonlinelibrary.com). DOI: 10.1002/jbm.b.33227

Abstract: With an increasingly aging population, a significant challenge in implantology is the creation of biomaterials that actively promote tissue integration and offer excellent mechanical properties. Engineered surfaces with micro- and nanoscale topographies have shown great potential to control and direct biomaterial–host tissue interactions. Two simple yet efficient chemical treatments, oxidative nanopatterning and anodization, have demonstrated the ability to confer exciting new bioactive capacities to commercially pure titanium and Ti–6Al–4V alloy. However, the resulting nanoporous and nanotubular surfaces require careful assessment in regard to potential adverse effects on the fatigue resistance, a factor which may ultimately cause premature failure of biomedical implants. In this work, we have investigated the impact of oxidative nanopatterning and anodization on the fatigue resistance of commercially pure titanium and Ti–6Al–4V. Quantitative (e.g., S-N curves) and qualitative analyses were carried out to precisely characterize the fatigue response of treated metals and compare it to that of polished controls. Scanning electron microscopy (SEM) imaging revealed the effects of cyclic loading on the fracture surface and on the structural integrity of chemically grown nanostructured oxides. Results from this study reinforce the importance of mechanical considerations in the development and optimization of micro- and nanoscale surface treatments for metallic biomedical implants. © 2014 Wiley Periodicals, Inc. J Biomed Mater Res Part B: Appl Biomater 00B:000–000, 2014.

Key Words: titanium, fatigue, oxidative nanopatterning, anodization, nanotopography

How to cite this article: Ketabchi A, Weck A, Variola F. 2014. Influence of oxidative nanopatterning and anodization on the fatigue resistance of commercially pure titanium and Ti–6Al–4V. J Biomed Mater Res Part B 2014:00B:000–000.

INTRODUCTION

Various strategies have been developed to control the cellular events that ultimately determine the biological outcome of biomedical implants.[1,2] It is now well established that the tissue integration of biomedical implants is governed by the micro- and nanoscale surface properties of materials, such as topography, roughness, surface chemistry, and potential.[1,3] It is therefore evident that achieving the capacity to precisely design the physicochemical properties of surfaces will ultimately result in the ability to guide the biological response to an implanted biomaterial. In this context, chemical treatments such as oxidative nanopatterning and anodization are very effective tools to endow titanium-based metals, the gold standard in implantology,[4–6] with the ability to control cellular events.[1,3] This unique capacity results from the creation of distinctive nanostructured oxide layers (sponge-like structures in the case of oxidative nanopatterning, nanotubular arrays in the case of anodization) capable of positively affecting cell activity.[7–10] Because these treatments showed promising *in vitro* results,[11,12] it is now important to determine whether the mechanical properties of modified metals are affected, thereby validating their applicability to *in vivo* applications (e.g., cardiovascular stents and orthopedic implants). The topographical modifications introduced by these two methods and, as a matter of fact, any technique which engenders new topographical features directly onto the surface, may in fact act as stress raisers that promote crack initiation and lead to a premature failure. Therefore, the effects of surface modification approaches will require mechanical validation before being applied to biomedical implants, usually subject to significant and complex stress fields.

In this context, fatigue failure is reported to account for about 90% of all failures in metals, polymers, and ceramics, and this extends to biomedical devices.[13] For instance, in dental implants, removable partial denture frameworks, clasps, plates, pedicle screws, and cables, fatigue is one of the main causes of failure.[4,14]

Several studies have evaluated the effects of various micro- and nanoscale surface modifications on the fatigue resistance of titanium based metals.[15–23] Among these, because of their excellent bioactive properties,[9,24] nanotubular structures generated by anodization on pure titanium and titanium alloys (e.g., Ti–6Al–7N and Ti–6Al–4V) have been investigated in relation to their influence on the fatigue behavior.[20,21] While no significant decrease in the

Correspondence to: A. Weck (e-mail: aweck@uottawa.ca)

TABLE I. Mechanical Properties of the cp-Ti and Ti–6Al–4V.[26]

Alloy	Tensile Strength (MPa)	Yield Strength (MPa)	Modulus of Elasticity (GPa)	RA (%)	Elongation (%)	Type of Alloy
cp-Ti (grade 2)	345	275	102.7	30	20	α
Ti–6Al–4V	895–930	825–869	110–114	20–25	6–10	$\alpha + \beta$

fatigue life of anodized commercially pure titanium was observed,[20] in the case of anodized Ti–6Al–7Nb and Ti–6Al–4V alloys the fatigue life was reduced.[22,23]

In this work, we carried out a quantitative and qualitative comparative evaluation of the effects of mechanical polishing, oxidative nanopatterning, and anodization on the fatigue behavior of both commercially pure titanium (cp-Ti) and Ti–6Al–4V. In particular, we addressed critical aspects of fatigue failure (e.g., S-N curves, fracture surface analysis), aiming at elucidating the fundamental metallurgical response of treated metals to a selectively chosen cyclic loading. In addition, distinctively from previous studies on the fatigue resistance of titanium and its alloys,[20–23] we have paid particular attention to surface phenomena (e.g., oxide layer damaging and exfoliation) which are important to validate the suitability of a particular treatment for biomedical implants. Although our goal was not to recreate and investigate the mechanical conditions that typically characterize biomedical implants (e.g., applied load, frequency and amplitude, and stress/strain rate), our results nonetheless contribute to provide important guidance for the rational design, optimization and implementation of micro- and nanoscale surface modification approaches for *in vivo* applications.

MATERIALS AND METHODS

Materials

Commercially pure grade 2 titanium (hereafter indicated as cp-Ti) and Ti–6Al–4V 3.175 mm × 91.5 cm rods (Titanium Industries, Montreal, QC, Canada) were utilized for this study. The mechanical properties of these metals are shown in Table I. The average grain size, assuming an equiaxed microstructure, was estimated by using Heyn Lineal Intercept Procedure provided by the American Society for Testing and Materials (ASTM) International standards designation E112-12.[25] The average size of the grains for cp-Ti and Ti–6Al–4V was 24 μm and 4 μm, respectively.

Sample design

Samples were machined according to the ASTM International Standards designation E466-07.[27] The final specimen design, with a radius of curvature of 20 mm at test section and outer diameter of 3 mm, is shown in Figure 1.

Surface modification techniques

Mechanical polishing. ASTM-compliant samples were mechanically polished to remove machining marks, undesired surface roughness and inhomogeneities to minimize their effects on the evaluation of the fatigue behavior. The polishing direction was perpendicular to the main axis of the dog bone-shaped specimens. A three-step polishing was carried out; first using 1200 grit and 4000 grit silicon carbide sandpapers and lastly using a cloth soaked in a mixture of 0.05 μm colloidal silica suspension and hydrogen peroxide. Polished samples were then used as a reference in the assessment of the fatigue resistance of chemically treated samples. As shown in previous work, polished samples exhibit an average roughness value of 50 nm and 7 nm for cp-Ti[28] and Ti–6Al–4V,[8] respectively. Because of the standardized design and geometry of the samples used in this study, we were not able to directly assess their roughness values. In particular, their nonplaneity made them not readily amenable to analytical techniques for surface roughness measurements, such as profilometric and atomic force microscopy measurements. We can however extrapolate that also for the samples used in this study, the average roughness values are expected to fall within the previously reported range.

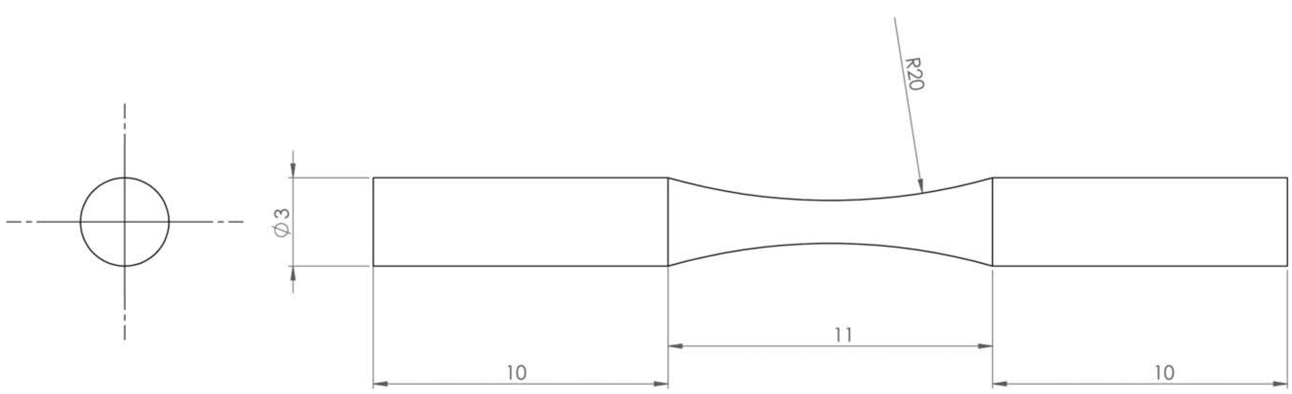

FIGURE 1. Specimen with continuous radius ($R = 20$ mm, $D = 1.5$ mm), designed based on ASTM International Standards for axial fatigue testing, designation E466-07.[27]

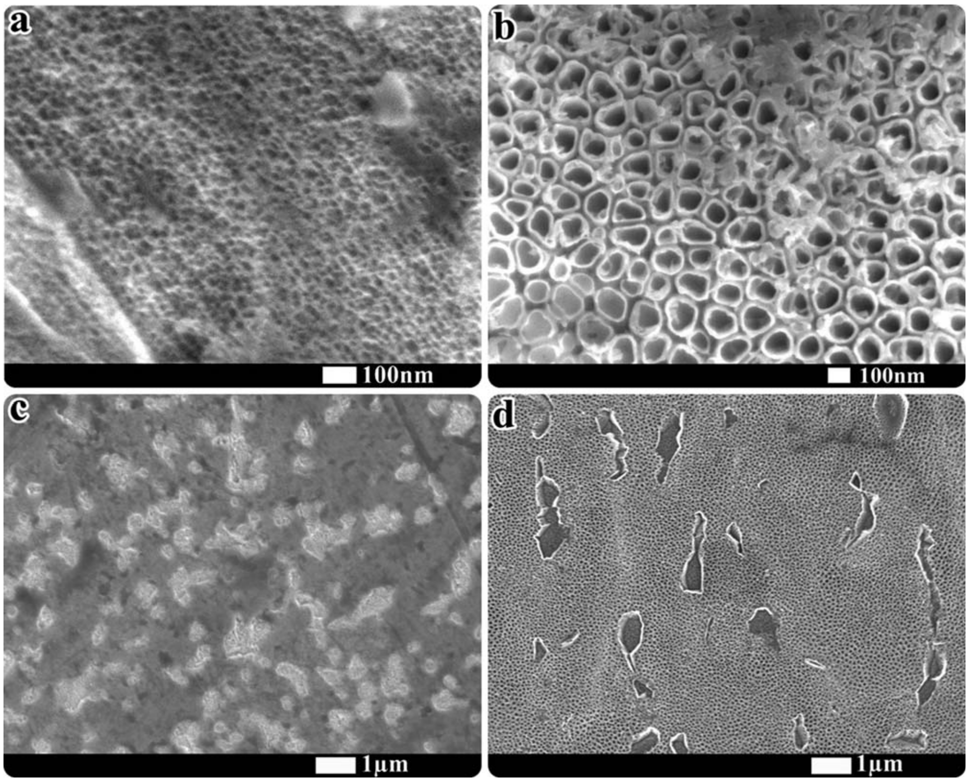

FIGURE 2. Nanopits and nanotubes created, respectively, by oxidative nanopatterning and anodization of cp-Ti (a,b) and Ti-6Al-4V (c,d). Preferentially etched β-phase grains appeared as microcracks on the surface of Ti–6Al–4V surface treated by oxidative nanopatterning (c) and anodization (d).

Chemical treatments. Oxidative nanopatterning and anodization were carried out according to published protocols.[29–32] In brief, in the case of oxidative nanopatterning, metallic samples were immersed in a 50:50 H_2SO_4/H_2O_2 solution for 2.5 h under moderate stirring, and successively rinsed in distilled water. In the case of anodization, samples (anode) were treated at 20 V for 30 min in an electrochemical cell composed by a stainless steel beaker (cathode) containing an 0.5% hydrofluoric acid solution. Previous work has extensively characterized cp-Ti and Ti–6Al–4V samples, treated by both oxidative nanopatterning[8,28] and anodization.[33–35] In the case of cp-Ti, these treatments impacted the topography mainly at the nanoscale. However, in the case of Ti–6Al–4V, a selective etching of β-grains engendered a submicrometric topography.

Fatigue testing equipment and procedure

For uniaxial fatigue testing, an Instron All-Electric ElectroPuls™ E3000 with a maximum dynamic capacity of ±3 kN and maximum frequency of 100 Hz was used. Data were processed and analyzed by the Wavematrix™ Software. Stress levels adopted in this study have been selectively chosen above the endurance limit of the metals. According to the cross sectional area of the sample, the required constant load amplitude was calculated. Uniaxial fully reversed (load ratio $R = -1$) fatigue test was carried out using sinusoidal waveforms. Because of the higher stresses required by the alloy, the frequency for axial fatigue test was 10 Hz and 5 Hz for cp-Ti and Ti–6Al–4V, respectively. At these frequencies, potential heating and, more generally, adverse effects solely related to such relatively low frequency values, are not expected to influence the fatigue results.[36,37]

Surface characterization

To investigate the nanotopographies created by oxidative nanopatterning and anodization, polished controls and treated samples were imaged by a Scanning Electron Microscope (JEOL, JSM-7500F). This allowed us (i) to assess the effects of cyclic loading on the integrity of the outer oxide layer and (ii) to reveal fatigue failure characteristics (e.g., beachmarks and striations). In particular, four images taken in each of the five positions along the sample corresponding to different stress levels were analyzed (Figures 8 and 9). The area fraction of delaminated nanotubes from the surface of the metal was quantified by using ImageJ software (NIH, Bethesda, Maryland) (Figure 10). The unpaired *t*-test (p value < 0.05) ensured statistical significance.

RESULTS

Chemical treatments

Oxidative nanopatterning of cp-Ti and Ti–6Al–4V engendered a sponge-like titanium dioxide (TiO_2) layer composed by a homogenous network of nanosized pits [Figure 2(a)], approximately 21 nm in diameter.[29,38] The physicochemical properties of the resulting surfaces have been characterized in detail elsewhere.[29,38] Anodized surfaces displayed uniformly

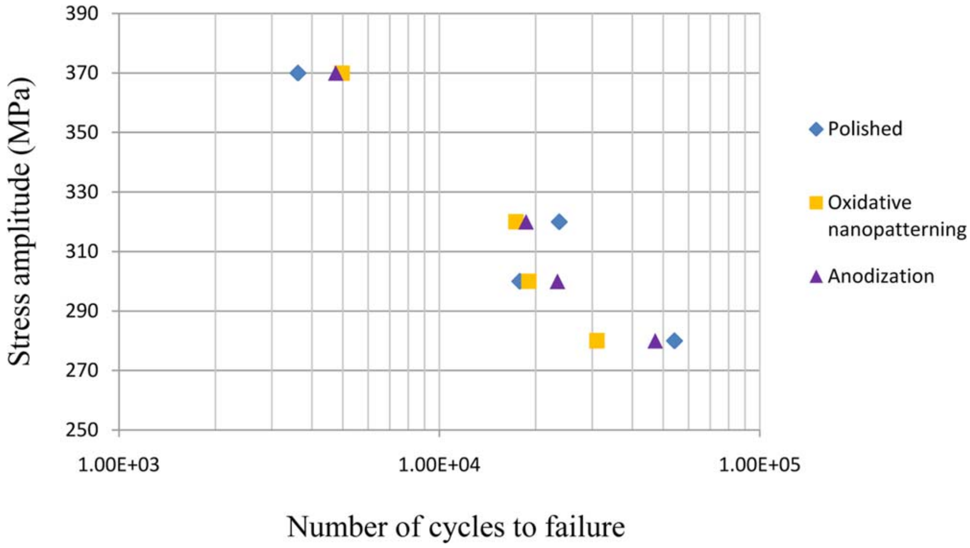

FIGURE 3. S-N curves for polished and chemically modified cp-Ti. Fatigue tests were conducted at four different stress levels for each surface treatment. The number of tests (i.e., points per curve) has been chosen to reflect previously published studies on the fatigue response of cp-Ti.[20] [Color figure can be viewed in the online issue, which is available at wileyonlinelibrary.com.]

distributed arrays of TiO_2 nanotubes [Figure 2(b)] whose average diameter and length were measured from the SEM images. The diameter resulted 86 ± 9 nm and 78 ± 6 nm, and the length was estimated to be 380 ± 16 nm and 210 ± 13 nm, for cp-Ti and Ti–6Al–4V, respectively. Microcavities resulting from the selective removal of the β-phase grains were observed in Ti–6Al–4V samples treated by both oxidative nanopatterning [Figure 2(c)] and anodization [Figure 2(d)], as previously reported.[38]

Fatigue behavior

S-N curves. Graphs showing the cyclic stress plotted against the number of cycles to failure (i.e., S-N curves) were obtained for both pristine and chemically modified metals. Consistently with previous work,[15,17,20–23] we generated S-N curves by carring out fatigue testing throughout a wide range of stress levels rather than focusing on multiple tests at one stress level. S-N curves display in fact a trend across stress levels rather than multiple measurements at one stress value, and therefore require several trials at different stresses. More precisely, for each surface treatment, four and five stress values were used for cp-Ti and Ti–6Al–4V, respectively (Figures 3 and 4). This also allowed us to compare our findings to published results. Statistical significance of such curves was ensured by the number of points chosen for each curve.[20,21]

In the case of treated samples, the resulting surface features did not significantly affect the fatigue resistance of cp-Ti

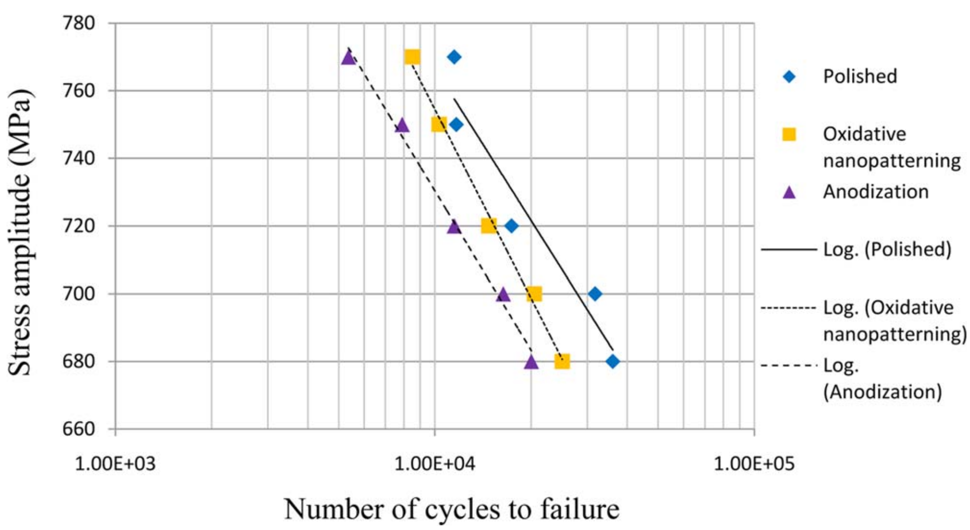

FIGURE 4. S-N curves for polished and chemically modified Ti–6Al–4V. Fatigue tests were conducted at five different stress levels for each surface treatment. The number of tests (i.e., points per curve) has been chosen to reflect previously published studies on the fatigue response of the Ti–6Al–4V.[21] [Color figure can be viewed in the online issue, which is available at wileyonlinelibrary.com.]

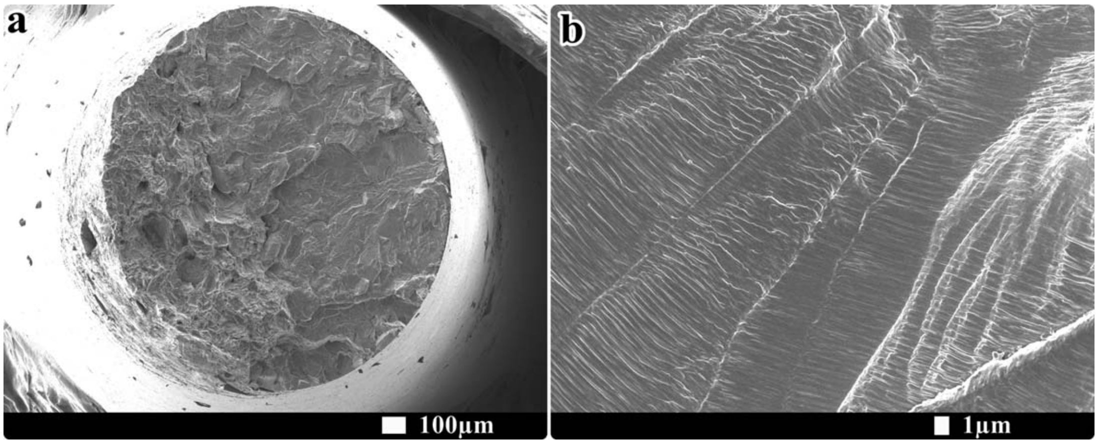

FIGURE 5. SEM images of the fracture surface of polished cp-Ti (cross sectional area). Beachmarks and striations are visible (b). These striations and beachmarks were observed on both untreated and treated samples.

(Figure 3). However, Figure 4 shows that the performance of the alloy was significantly influenced by the surface treatments. In particular, the S-N curves indicate that, compared to polished samples, both oxidative nanopatterning and anodization impacted negatively its fatigue resistance, with more deleterious effects associated to the former technique.

Morphological and fractured surface analysis

Although S-N curves provide valuable information about the fatigue behavior, further analyses were required to investigate morphological and structural changes occurring in both the bulk metal and the outer nanostructured oxide in response to cyclic loading. In particular, SEM imaging of fractured surfaces was used to investigate crack nucleation, propagation paths and fatigue failure characteristics. This analysis also identified beachmarks and striations [Figure 5(b)], thereby providing clear evidence of fatigue failure. However, no significant differences in terms of fracture surface morphologies were detected after the chemical treatments, suggesting that the differences in fatigue life were solely due to surface effects.

In the case of oxidative nanopatterning, surface microcracks were observed in the bulk metal (Figure 6). However, we could not detect any apparent modification of the oxide layer. Conversely, in the case of anodized samples, significant damaging of the oxide layer was evident. Initial isolated cracks eventually joined together in regions where the stress values were higher. In fact, as the distance to the fracture surface decreased, cracks increased in number and size (Figure 7). This ultimately yielded significant exfoliation of the oxide layer, creating islands of adherent and intact nanotubes surrounded by the bare metallic surface. In the case of cp-Ti, the first cracks were observed at positions corresponding to 237 ± 28 MPa. These values significantly increased to 658 ± 28 MPa for anodized Ti–6Al–4V samples.

Effects of cyclic loading on the anodized oxide layer

In the case of anodized samples, the effects of cyclic loading on the nanotubular oxide layer were also assessed by evaluating the area fraction of pristine versus cracked nanotubes. Compared to the alloy, a higher fraction of nanotubes delaminated off the surface of cp-Ti. In addition, a significant decrease in area fraction of intact nanotubes was observed on cp-Ti toward the fracture surface. However, variations in area fraction of intact nanotubes on the surface of Ti–6Al–4V were not statistically significant.

DISCUSSION

In this article, we assessed the effects of oxidative nanopatterning and anodization on the fatigue resistance of titanium

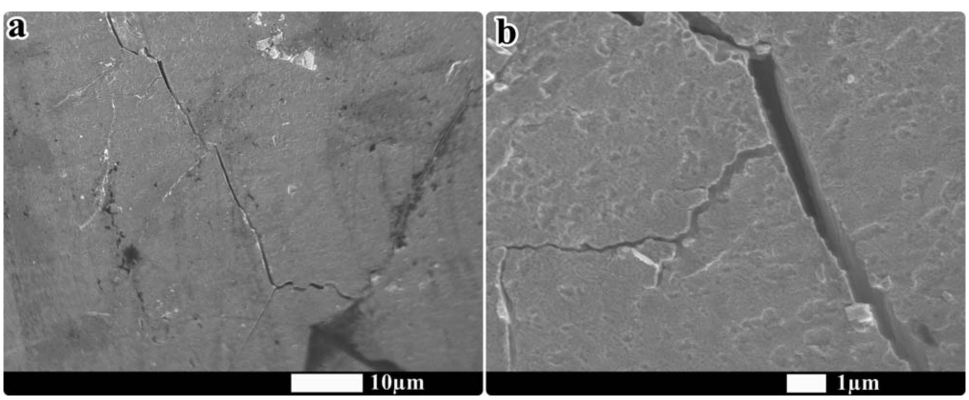

FIGURE 6. Scanning electron micrographs of cp-Ti samples subjected to oxidative nanopatterning. Fracture in the bulk metals can be observed.

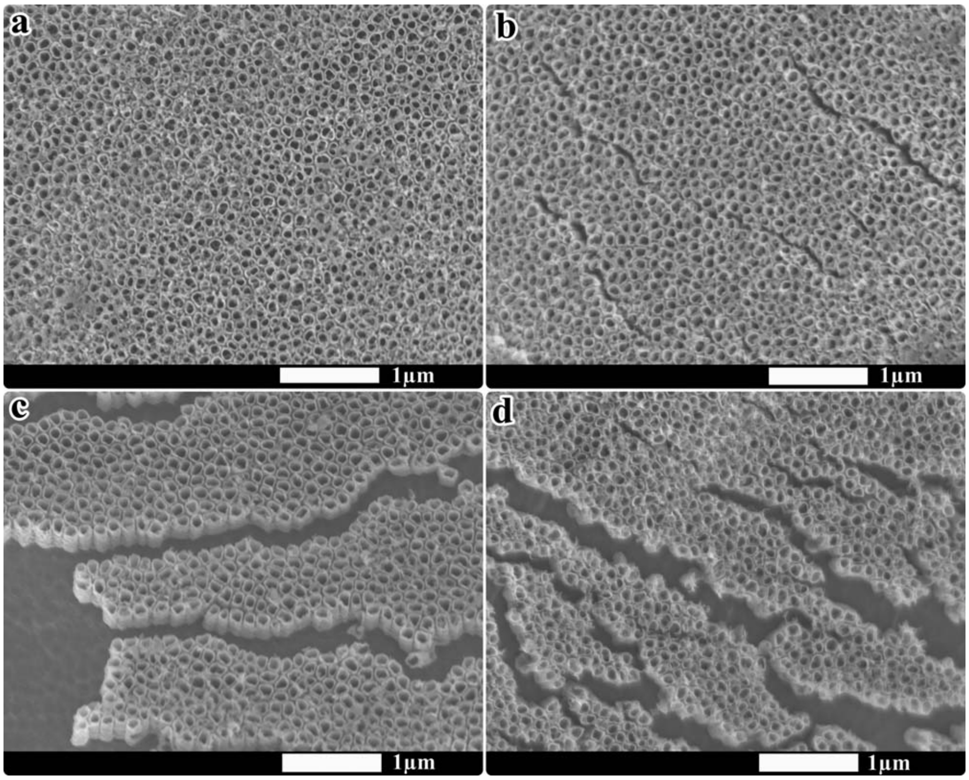

FIGURE 7. Scanning electron micrographs illustrating the effects of cyclic loads on the cp-Ti oxide layer created by anodization as increasingly moving from the farthest point (a) to the closest point (d) to the fracture surface. Small cracks initiated and developed along the walls of nanotubes at sites distant from the fracture (b) and increased in number and size as moving closer to the fracture surface (c and d).

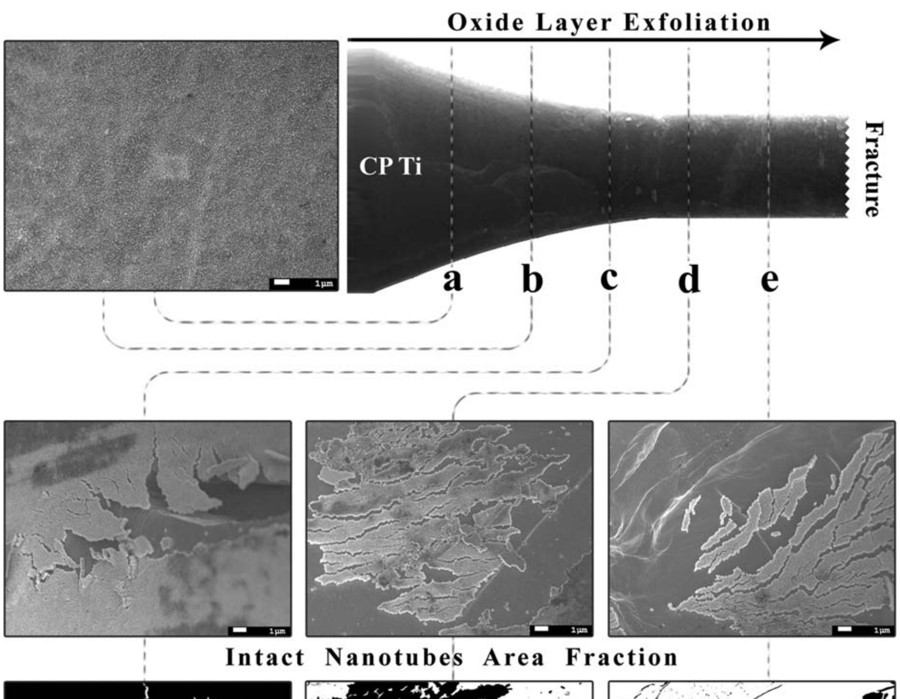

FIGURE 8. Morphological analysis of the nanotubular oxide layer grown on cp-Ti as a function of the position along the sample. Intact nanotubes (a and b), onset and propagation of exfoliation (c and d), and exfoliation close to the fracture surface (e).

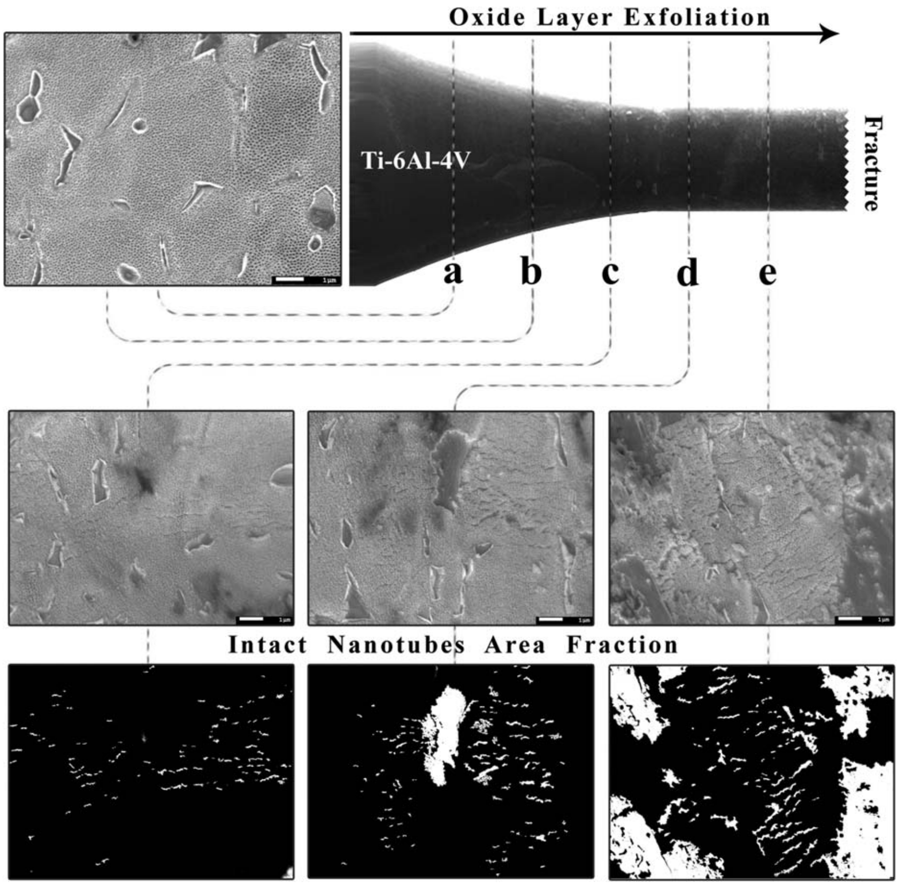

FIGURE 9. Morphological analysis of the nanotubular oxide layer grown on the Ti–6Al–4V alloy as a function of the position along the sample. Intact nanotubes (a and b), onset and propagation of exfoliation (c and d), and exfoliation close to the fracture surface (e).

based metals. Consistently with a previous work for axial fatigue testing,[20] the S-N curves demonstrate that nanoscale surface treatments do not significantly affect the fatigue resistance of cp-Ti. In particular, our results indicate that structural damages of the oxide layer do not affect the fatigue response of the bulk metal (Figure 7). Similarly, in the case of the alloy, our findings confirm that nanoscale surface treatments decrease the fatigue life.[22,23] This is believed to be related to the combined effects of the more brittle,[23] and heterogeneous TiO_2 layer that includes Al_2O_3 and V_2O_5,[38] the presence of pre-existing microcracks in the oxide and the accumulation of internal stresses during the oxidation process.[23] Therefore, if cracks in the nanostructured oxide had been responsible of the decreased fatigue life of the alloy, we would have undoubtedly observed a difference in the fatigue behavior of cp-Ti as well. Taken together, these considerations suggest that the fatigue failure cannot be solely associated to the creation of nanoscale topographical features in oxide layer, but to additional effects.

The lower fatigue resistance of Ti–6Al–4V by both treatments was attributed to metallurgical factors, in particular to the biphasic ($\alpha + \beta$) nature of the alloy (as opposed to the monophasic structure of cp-Ti). When in contact with the etching solution, a selective etching of the more reactive β-phase grains (as compared to the α-phase) occurs.[38] Such differential attack creates microscale crevices that extend inwards toward the underlying metals [Figure 2(c,d)]. These microcavities are believed to act as stress concentration sites which initiate crack nucleation and propagation upon cyclic loading until fatigue failure. Because such selective attack only occurs in the alloy, we inferred that it may be the main cause of the observed variations in the fatigue resistance (Figure 4).

While in the case of oxidative nanopatterning no apparent alteration of the outer oxide layer was observed (likely because of its relatively thinner thickness, in the 30–50 nm range[29]), the analysis of the integrity of nanotubular oxide layer (Figures 8 and 9) revealed exfoliation/delamination, exhibiting a more pronounced tendency on cp-Ti (Figure 10). Such phenomenon has a direct relationship with the position along the sample and thus the stress level, with more intense effects close to the fracture surface where the stress is higher. Furthermore, higher stresses also imply a higher strain which in turn promotes the creation of a mismatch between the deformation of the oxide layer and that of the underlying metal, ultimately causing delamination.

The observed differences in the structural behavior of the oxides grown on the two metals may call for additional factors, such as a greater thickness (i.e., 380 ± 16 nm for cp-Ti and 210 ± 13 nm for Ti–6Al–4V), lower strength and adhesion,[39,40] and higher brittleness[23] of the oxide on cp-Ti.

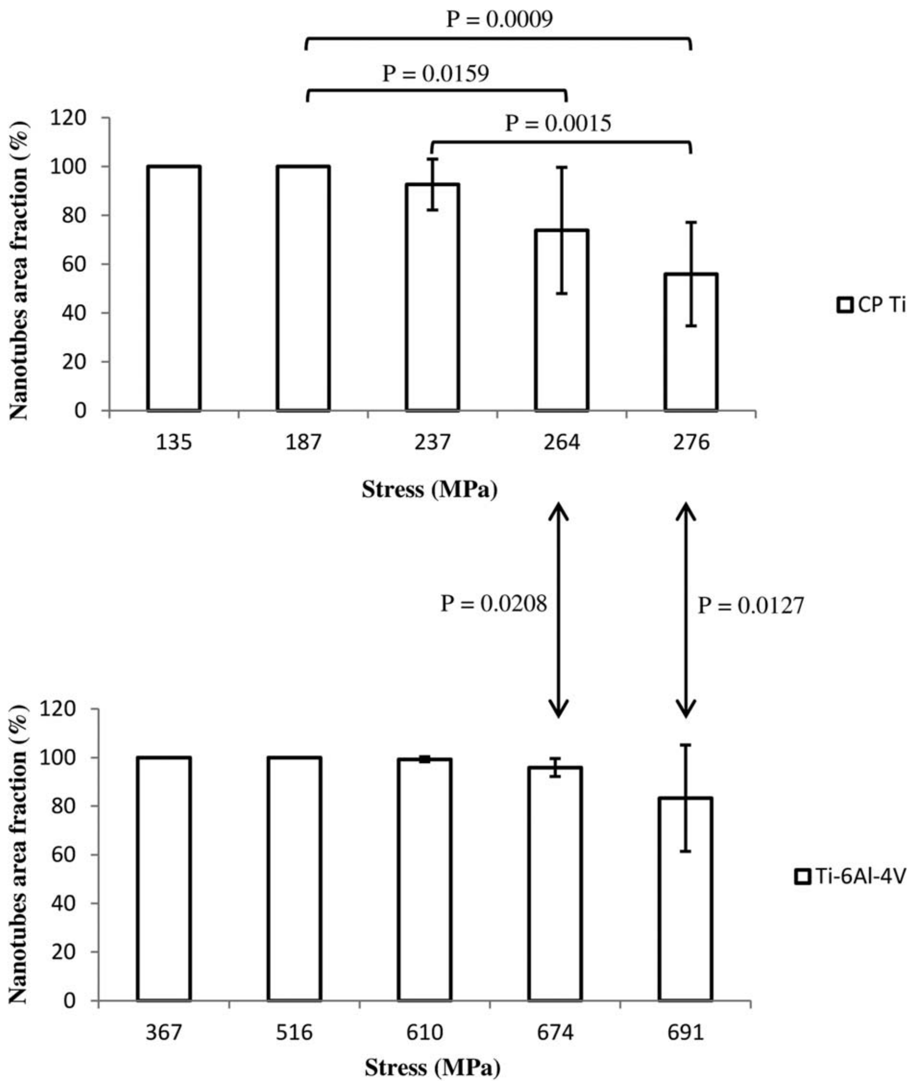

FIGURE 10. Area fraction of intact nanotubes, calculated as the ratio between the surface of intact nanotubes and the total surface. Stress values (*x*-axis) increase toward the fracture surface. Four images were analyzed for each of the five stress levels and error bars are provided.

In this context, we would like to point out that in this work we only used one set of experimental parameters for anodization, selectively chosen according to *in vitro* studies.[32] The characteristics of the nanotubular oxide layer (e.g., nanotube diameter and length) are known to vary greatly according the treatment parameters.[31,34] Therefore, the thickness of the nanostructured oxide, as well as other physicochemical properties that can determine its susceptibility to delamination (e.g., crystallinity), can be optimized to limit/avoid exfoliation. In addition, because (i) the main goal of this study was to compare the effects of different surface treatments on the intrinsic metallurgical properties of the metals and (ii) the time needed for fatigue measurements required accelerated tests, the stresses chosen in this study (as well as the resulting strains) may be higher than those normally observed in biomedical implants. In this context, it will be interesting (i) to reproduce the precise stress fields that develop in *in vivo* applications and (ii) to carry out the experiments in simulated bodily fluid environments (known to accelerate fatigue failure[41,42]) in order to better assess how the effects described herein will translate to the clinical setting.

CONCLUSION

In this work, we have demonstrated that oxidative nanopatterning and anodization do not have significant effects on the fatigue resistance of cp-Ti. However, in the case of the Ti–6Al–4V alloy, our results show that these nanoscale surface treatments negatively impact its fatigue life. It was inferred that the primary cause of such a detrimental effect is the preferential etching of the β-phase grains, which resulted in the formation of microcavities that facilitate crack nucleation at a lower stress. In addition, our findings also demonstrate that the decrease in fatigue resistance of the alloy was more pronounced in case of anodization. Exfoliation rate of the nanotubular oxide layer as a function of distance to fracture surface was found to be higher for cp-Ti as compared to the alloy. This outcome was attributed to the greater thickness, lower strength and adhesion,[39,40] and higher brittleness[23] of the oxide layer formed on cp-Ti. In addition, we have shown that, depending on the experimental parameters (which in turn determine the physicochemical makeup of the outer oxide layer), the nanotubular oxide layer may undergo exfoliation, thereby reinforcing the necessity of careful selection and optimization of treatment parameters before translating *in vitro* results to the *in vivo* reality.

ACKNOWLEDGMENTS

Dr. Variola acknowledges start-up funding from the University of Ottawa and Faculty of Engineering. Dr. Weck gratefully acknowledges the support of the Natural Sciences and Engineering Research Council of Canada (NSERC).

REFERENCES

1. Variola F, Brunski J, Orsini G, de Oliveira PT, Wazen R, Nanci A. Nanoscale surface modifications of medically-relevant metals: State-of-the art and perspectives. Nanoscale 2011;3:335–353.
2. Tran N, Webster TJ. Nanotechnology for bone materials. Wiley Interdiscip Rev Nanomed Nanobiotechnol 2009;1:336–351.
3. Variola F, Vetrone F, Richert L, Jedrzejowski P, Yi JH, Zalzal S, Clair S, Sarkissian A, Perepichka DF, Wuest JD, Rosei F, Nanci A. Improving biocompatibility of implantable metals by nanoscale modification of surfaces: An overview of strategies, fabrication methods, and challenges. Small 2009;5:996–1006.
4. Noort RV. Titanium: The implant material of today. J Mater Sci 1987;22:3801–3811.
5. Rack HJ, Qazi JI. Titanium alloys for biomedical applications. Mater Sci Eng C 2006;26:1269–1277.
6. Lütjering G, Williams JC. Titanium. New York: Springer; 2007. 449 pp.
7. Vetrone F, Variola F, Tambasco de Oliveira P, Zalzal SF, Yi JH, Sam J, Bombonato-Prado KF, Sarkissian A, Perepichka DF, Wuest JD, Rosei F, Nanci A. Nanoscale oxidative patterning of metallic surfaces to modulate cell activity and fate. Nano Lett 2009;9:659–665.
8. Richert L, Vetrone F, Yi J-H, Zalzal SF, Wuest JD, Rosei F, Nanci A. Surface nanopatterning to control cell growth. Adv Mater 2008; 20:1488–1492.
9. Das K, Bose S, Bandyopadhyay A. TiO_2 nanotubes on Ti: Influence of nanoscale morphology on bone cell–materials interaction. J Biomed Mater Res A 2009;90A:225–237.
10. Yu W, Jiang X, Zhang F, Xu L. The effect of anatase TiO_2 nanotube layers on MC3T3-E1 preosteoblast adhesion, proliferation, and differentiation. J Biomed Mater Res A 2010;94A:1012–1022.
11. De Oliveira PT, Zalzal SF, Beloti MM, Rosa AL, Nanci A. Enhancement of in vitro osteogenesis on titanium by chemically produced nanotopography. J Biomed Mater Res A 2007;80A:554–564.
12. Popat KC, Leoni L, Grimes CA, Desai TA. Influence of engineered titania nanotubular surfaces on bone cells. Biomaterials 2007;28: 3188–3197.
13. Teoh S. Fatigue of biomaterials: A review. Int J Fatigue 2000;22: 825–837.
14. Hermawan H. Biodegradable Metals: From Concept to Applications. New York: Springer; 2012. 73 pp.
15. Pazos L, Corengia P, Svoboda H. Effect of surface treatments on the fatigue life of titanium for biomedical applications. J Mech Behav Biomed Mater 2010;3:416–424.
16. Vallittu PK, Kokkonen M. Deflection fatigue of cobalt-chromium, titanium, and gold alloy cast denture clasp. J Prosthet Dent 1995; 74:412–419.
17. Laonapakul T, Otsuka Y, Nimkerdphol AR, Mutoh Y. Acoustic emission and fatigue damage induced in plasma-sprayed hydroxyapatite coating layers. J Mech Behav Biomed Mater 2012;8:123–133.
18. Costa MYP, Venditti MLR, Voorwald HJC, Cioffi MOH, Cruz TG. Effect of WC–10%Co–4%Cr coating on the Ti–6Al–4V alloy fatigue strength. Mater Sci Eng A 2009;507:29–36.
19. Le Guéhennec L, Soueidan A, Layrolle P, Amouriq Y. Surface treatments of titanium dental implants for rapid osseointegration. Dent Mater 2007;23:844–854.
20. Leinenbach C, Eifler D. Influence of oxidation treatment on fatigue and fatigue-induced damage of commercially pure titanium. Acta Biomater 2009;5:2810–2819.
21. Leinenbach C, Eifler D. Fatigue and cyclic deformation behaviour of surface-modified titanium alloys in simulated physiological media. Biomaterials 2006;27:1200–1208.
22. Costa MYP, Voorwald HJC, Pigatin WL, Guimarães VA, Cioffi MOH. Evaluation of shot peening on the fatigue strength of anodized Ti–6Al–4V alloy. Mater Res 2006;9:107–109.
23. Apachitei I, Lonyuk B, Fratila-Apachitei LE, Zhou J, Duszczyk J. Fatigue response of porous coated titanium biomedical alloys. Scripta Mater 2009;61:113–116.
24. Das K, Bose S, Bandyopadhyay A, Karandikar B, Gibbins BL. Surface coatings for improvement of bone cell materials and antimicrobial activities of Ti implants. J Biomed Mater Res B Appl Biomater 2008;87B:455–460.
25. ASTM Standard E112, 2013, Standard Test Methods for Determining Average Grain Size, ASTM International, West Conshohocken, PA, 2014, DOI: 10.1520/E0112-13, Available from: http://www.astm.org.
26. Niinomi M. Mechanical properties of biomedical titanium alloys. Mater Sci Eng A 1998;243:231–236.
27. ASTM Standard E466, 2007, Standard Practice for Conducting Force Controlled Constant Amplitude Axial Fatigue Tests of Metallic Materials, ASTM International, West Conshohocken, PA, 2007, DOI: 10.1520/E0466-07, Available from: http://www.astm.org.
28. Ketabchi A, Komm K, Miles-Rossouw M, Cassani DAD, Variola F. Nanoporous titanium surfaces for sustained elution of proteins and antibiotics. PLoS One 2014;9:e92080.
29. Yi J-H, Bernard C, Variola F, Zalzal SF, Wuest JD, Rosei F, Nanci A. Characterization of a bioactive nanotextured surface created by controlled chemical oxidation of titanium. Surf Sci 2006;600:4613–4621.
30. Variola F, Lauria A, Nanci A, Rosei F. Influence of treatment conditions on the chemical oxidative activity of H_2SO_4/H_2O_2 mixtures for modulating the topography of titanium. Adv Eng Mater 2009; 11:B227–B234.
31. Brammer KS, Oh S, Cobb CJ, Bjursten LM, Heyde H van der, Jin S. Improved bone-forming functionality on diameter-controlled TiO_2 nanotube surface. Acta Biomater 2009;5:3215–3223.
32. Ercan B, Taylor E, Alpaslan E, Webster TJ. Diameter of titanium nanotubes influences anti-bacterial efficacy. Nanotechnology 2011;22:295102.
33. Demetrescu I, Ionita D, Pirvu C, Portan D. Present and future trends in TiO_2 nanotubes elaboration, characterization and potential applications. Mol Cryst Liq Cryst 2010;521:195–203.
34. Minagar S, Berndt CC, Wang J, Ivanova E, Wen C. A review of the application of anodization for the fabrication of nanotubes on metal implant surfaces. Acta Biomater 2012;8:2875–2888.
35. He P, Chen K, Yu B, Yue CY, Yang J. Surface microstructures and epoxy bonded shear strength of Ti6Al4V alloy anodized at various temperatures. Compos Sci Technol 2013;82:15–22.
36. Morrissey RJ, Nicholas T. Fatigue strength of Ti–6Al–4V at very long lives. Int J Fatigue 2005;27:1608–1612.
37. Ritchie RO, Davidson DL, Boyce BL, Campbell JP, Roder O. High-cycle fatigue of Ti–6Al–4V. Fract Eng Mater Struct 1999;22: 621–31.
38. Variola F, Yi J-H, Richert L, Wuest JD, Rosei F, Nanci A. Tailoring the surface properties of Ti6Al4V by controlled chemical oxidation. Biomaterials 2008;29:1285–1298.
39. Adachi M, Mackert JR, Parry EE, Fairhurst CW. Oxide adherence and porcelain bonding to titanium and Ti–6A1–4V alloy. J Dent Res 1990;69:1230–1235.
40. Szmukler-Moncler S, Testori T, Bernard JP. Etched implants: A comparative surface analysis of four implant systems. J Biomed Mater Res B Appl Biomater 2004;69B:46–57.
41. Fleck C, Eifler D. Corrosion, fatigue and corrosion fatigue behaviour of metal implant materials, especially titanium alloys. Int J Fatigue 2010;32:929–935.
42. Zavanelli RA, Pessanha Henriques GE, Ferreira I, de Almeida Rollo JMD. Corrosion-fatigue life of commercially pure titanium and Ti–6Al–4V alloys in different storage environments. J Prosthet Dent 2000;84:274–279.